Semiconductor Science and Technology

Thin films of arsenic sulfide by chemical deposition and formation of InAs

To cite this article: Y Peña-Méndez *et al* 2006 *Semicond. Sci. Technol.* **21** 450

INSTITUTE OF PHYSICS PUBLISHING SEMICONDUCTOR SCIENCE AND TECHNOLOGY

Semicond. Sci. Technol. **21** (2006) 450–461 doi:10.1088/0268-1242/21/4/007

Thin films of arsenic sulfide by chemical deposition and formation of InAs

Y Peña-Méndez, M T S Nair and P K Nair

Department of Solar Energy Materials, Centro de Investigación en Energía, Universidad Nacional Autónoma de México, Temixco, Morelos-62580, Mexico

E-mail: mtsn@cie.unam.mx

Received 4 September 2005, in final form 30 January 2006
Published 24 February 2006
Online at stacks.iop.org/SST/21/450

Abstract

We report a method for obtaining thin films of arsenic sulfide by chemical bath deposition and the subsequent formation of InAs by heating the films with a vacuum-deposited coating of In. X-ray diffraction (XRD) studies have shown that the thin film deposited from chemical baths of pH ∼2, prepared by mixing aqueous acidic solutions of As(III) with sodium thiosulfate, is a composite film of crystalline As_2O_3 and As_2S_3, with the incorporation of sulfur. When heated at 150–250 °C, the As_2O_3 component transforms to As_2S_3, but still with very few identifiable peaks in the XRD patterns of the annealed samples. The films have a direct band gap of ≈2.7 eV (as-prepared) and ≈2.52 eV (heated at 250 °C), with forbidden optical transitions. The sheet resistance of the film (300 nm thick) is 10^{12} Ω, and the electrical conductivity is 10^{-8} Ω^{-1} cm^{-1}. After being heated in a sulfur-rich atmosphere at >200 °C, the films show photosensitivity. The As_2O_3/As_2S_3 thin film with an evaporated indium film, when heated at 250 °C in nitrogen or air, produces InAs as a major crystalline component. In this case, In_2S_3 or In_2O_3 may be present as a minor component in the films, depending on whether heating is done in nitrogen or air, respectively. The optical band gap of this InAs component is direct, 0.5 to 0.8 eV, depending on the film thickness and heating process. These composite films are photosensitive; a dark conductivity of 0.05 Ω^{-1} cm^{-1} in the films formed in nitrogen is ascribed to InAs and 5 Ω^{-1} cm^{-1} in the films formed by heating in air is ascribed to the In_2O_3 component. The photoconductivity of the films is of the same order of magnitude as the dark conductivity in each case.

1. Introduction

Arsenic sulfide is known for its photo-induced structural and optical changes, which has led to its application in optical imaging, hologram recording, electro-optic information storage devices and optical mass memories. Focusing on these applications, thin films of the material have been prepared by vacuum evaporation [1, 2], physical vapour deposition [3], spin coating [4], electrodeposition [5] and chemical deposition methods [6, 7], and their characteristics are reported. Pulsed laser deposition of As_2S_3 thin films for waveguide applications [8] and the temperature dependence of holographic recording in vacuum evaporated arsenic sulfide thin films on chromium-coated glass substrates [9] have also been reported.

Among the chalcogenides of group V elements with composition V_2VI_3, the energy gaps (E_g) vary from 2.6 eV for As_2S_3 to 0.16 eV for Bi_2Te_3 [10, 11]. Either n- or p-type conductivities may be obtained in these materials by controlled deviations from exact stoichiometry [10]. Optical band gaps in some of the V_2VI_3 compounds fall in a range appropriate for their use as absorber components in polycrystalline thin film solar cells: Sb_2S_3–$CuSbS_2$ [12], in which $CuSbS_2$ or alternately Cu_3SbS_4 was produced by heating Sb_2S_3–CuS layers [13, 14] and Sb_2S_3–$AgSbSe_2$, where $AgSbSe_2$ was produced by heating Sb_2S_3–Ag in Se-vapour [15]. We also reported that heating Sb_2S_3–In layers at 200–300 °C results in InSb [16]. Overall, our work on chemically deposited semiconductor thin films is mainly oriented towards large area coatings for solar

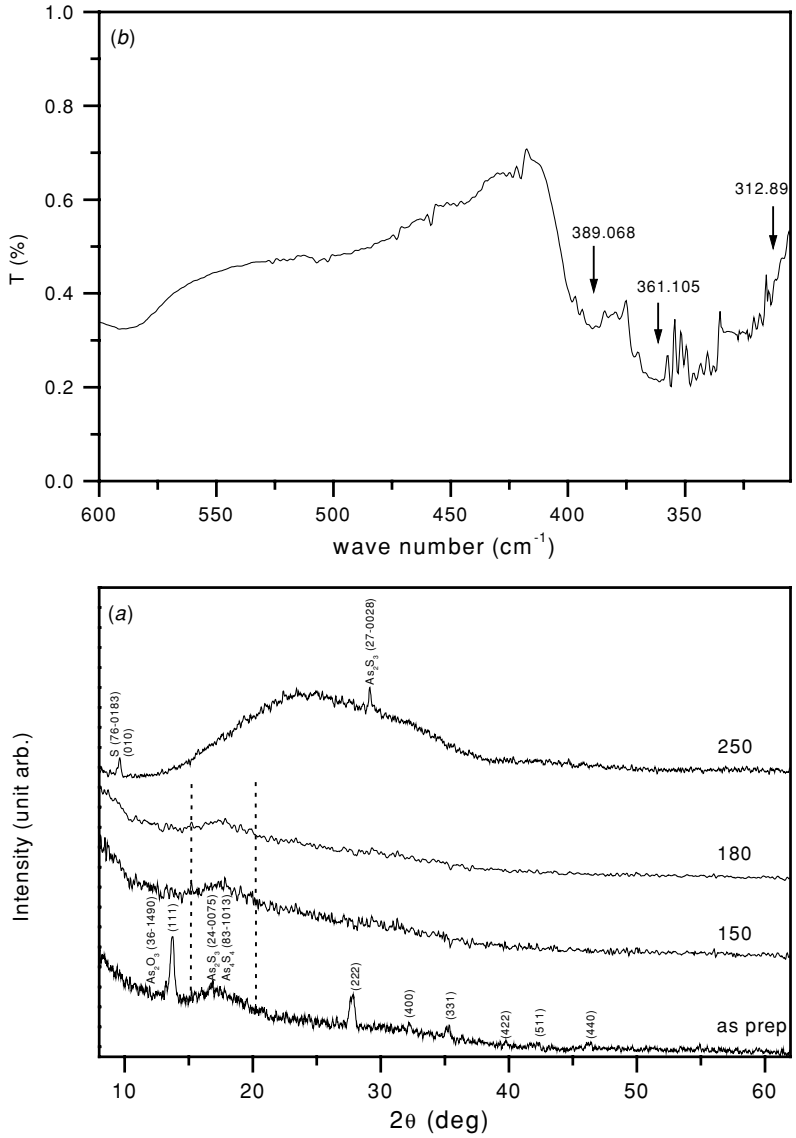

Figure 1. (*a*) XRD patterns of arsenic sulfide films, identifying the As_2O_3 component in the as-prepared film and assigning the observed peaks for the samples heated; (*b*) FTIR spectra of the arsenic sulfide precipitate obtained from the chemical deposition bath.

energy applications [17]. The present work on chemically deposited arsenic sulfide (As_2S_3) thin films has also been motivated by the versatility offered by chemically deposited bismuth sulfide [18, 19], bismuth selenide [20] and antimony selenide [21] with prospects for producing I–V–VI or III–V compounds for photoconductive or photovoltaic applications. However, they would have a wide range of applications wherever large area coatings of these materials are required at a comparatively low cost on a choice of electrically conductive or non-conductive planar, porous or nanostructured substrates or templates [22].

We report here that adherent and specularly reflective thin films of arsenic sulfide of thickness 300 nm can be deposited on glass substrates treated with organosilane, in a similar manner as reported previously for depositing adherent Bi_2S_3 thins films [23]. Structural, optical and electrical characteristics will be presented. We report the formation of InAs through heating an As_2S_3–In layer either in air or nitrogen, essentially following the same methodology as reported by us in producing InSb films [16]. We also noted that in a previous work on amorphous As_2S_3 thin films, it was reported that InAs is formed between As_2S_3 and In contact [24]. We shall present the optical and electrical characteristics of InAs films formed with some amount of In_2S_3 or In_2O_3, depending on whether the layer was heated in nitrogen or air. The procedure adopted here offers a relatively less expensive, large area method for producing III–V/III–VI composite thin films for distinct applications.

2. Experimental details

2.1. Chemical bath deposition of As_2S_3 thin films

2.1.1. Substrates. The deposition was carried out on Corning microscope glass slides (75 mm × 25 mm × 1 mm thickness) that were cleaned in detergent solution and water and treated

in a solution of organosilane in a similar way as reported in [23]. For this treatment, a solution of organosilane was prepared by adding 2 ml of *N*-[3-(trimethoxysilyl)-propyl]aniline, $C_{12}H_{21}NO_3Si$ (Aldrich) to a mixture of 90 ml of methanol and 10 ml of water. The resulting mixture was heated at 50 °C for 30 min with stirring and afterwards the glass slides were kept immersed in this hot solution for 1 h. The glass slides were then dried at 80 °C for 30 min and utilized for the chemical deposition of films. The role of organosilane in building covalent bonds to glass surface which would thus serve as a coupling agent for a successive coating and the optimum conditions for substrate treatment have been discussed earlier by many authors [25].

2.1.2. Solution of arsenic(III). A weighed quantity (1.9784 g) of arsenic(III) oxide, As_2O_3 (Spectrum Chemicals, 99.5–100.05 assay), was dissolved in a small quantity of water with an addition of 8 ml of concentrated HCl. Subsequently, the volume was made up to 100 ml in a volumetric flask by adding deionized water.

2.1.3. Deposition of the thin films. A deposition bath was prepared by adding with stirring 20 ml of 1 M solution of sodium thiosulfate, $Na_2S_2O_3{\cdot}5H_2O$ (Baker Analyzed Reagent), to 40 ml of the As(III) solution taken in a 100 ml beaker, and the volume was made up to 100 ml. The starting pH of this solution is 2. Glass slides treated in organosilane were placed in the bath with a slight inclination against the wall of the beaker and maintained at 35 °C in a circulation bath. The substrates were coated with films, which appear yellow in transmitted light and different tones of colour in reflection as the deposition proceeds. The typical duration of deposition was 6 h. The films were washed well with deionized water and dried. Specularly reflective thin films deposited on the side of glass slide that faced the wall of the beaker during the deposition were kept for analysis; the films on the other side were removed by scrubbing with cotton swabs moistened in HCl and subsequently with methanol to remove any organosilane residue.

Thickness measurements. Film thickness was measured using Alpha Step 100 (Tencor, CA). A slit was opened to serve as a step by scraping off the film from the substrate with a sharp splint. The thickness of the film deposited for 6 h in the bath was 300 nm. An estimate of the thin film yield was made using depositions on an array of substrates held together at a separation of 2 mm between each other. An acrylic lid with equidistant slots held the substrates vertically inside the bath. From the volume of the solution held between pairs of substrates and the thickness of the films, the thin film yield was estimated as 16%. This is the percentage of As in the bath recovered as As_2S_3 (or as a composite As_2O_3/As_2S_3; see section 3) thin film, evaluated following the procedure reported in [26]. The deposition technique may be improved further to reduce the precipitation and hence improve the thin film yield. Basically at small substrate separations, <1 mm, thin film yield $>50\%$ may be achieved, though the maximum film thickness would be typically <100 nm [27].

2.2. Vacuum evaporation of In

Glass substrates coated with arsenic sulfide thin films of thickness 300 nm were mounted on the substrate assembly,

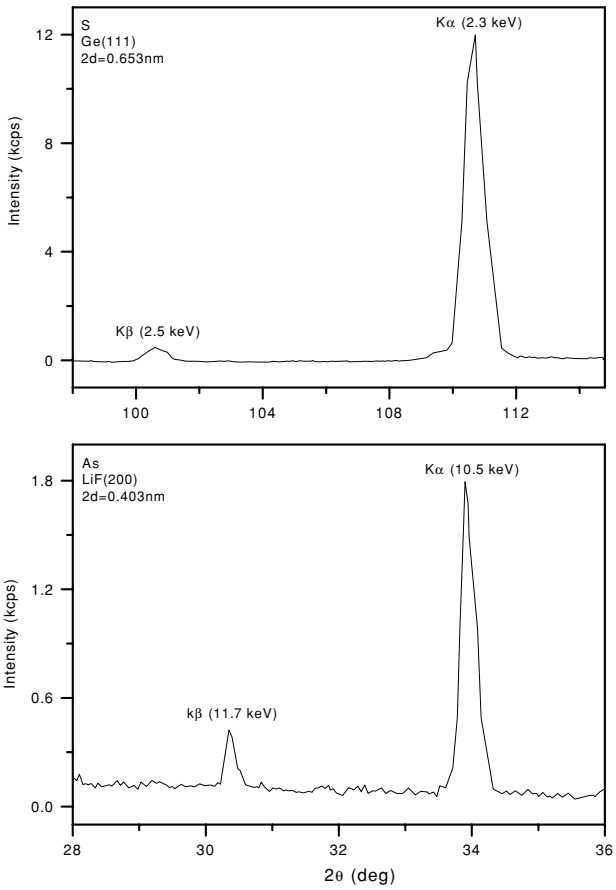

Figure 2. XRF spectra indicating the location of S and As peaks for the as-deposited film of As_2S_3/As_2O_3, 300 nm in thickness.

14 cm above a molybdenum boat in a thermal evaporation unit. A weighed quantity (5, 16 or 50 mg) of 99.999% purity indium wire (Aldrich) was placed in the molybdenum boat. After evacuating the chamber to a pressure of 10^{-6} mbar, the boat was heated to evaporate the indium completely. As the In film was soft, Alpha Step thickness measurement was not suitable. Film thickness was estimated using the deposition geometry, allowing for the directionality of the crucible: $\approx$15, 50 and 150 nm of In deposited on the As_2S_3 film by evaporating 5, 16 and 50 mg, respectively, of In.

Heat treatment of the films Samples of the films of arsenic sulfide deposited from the bath above were heated in air and nitrogen at different temperatures: 150 to 250 °C for 30 min each. Heating in air was done in a Lindberg furnace while that in nitrogen was done in a vacuum oven of T-M vacuum products. For annealing in nitrogen, the chamber was evacuated to 20 mTorr with the samples in, and subsequently nitrogen was introduced to increase the pressure up to 400 mTorr before raising the temperature of the furnace to the required value. The flow of nitrogen was maintained through the 30 min heating of the sample after attaining the temperature.

2.3. Characterization

X-ray diffraction (XRD) patterns of the films, for both as-prepared and after annealing, were recorded on a

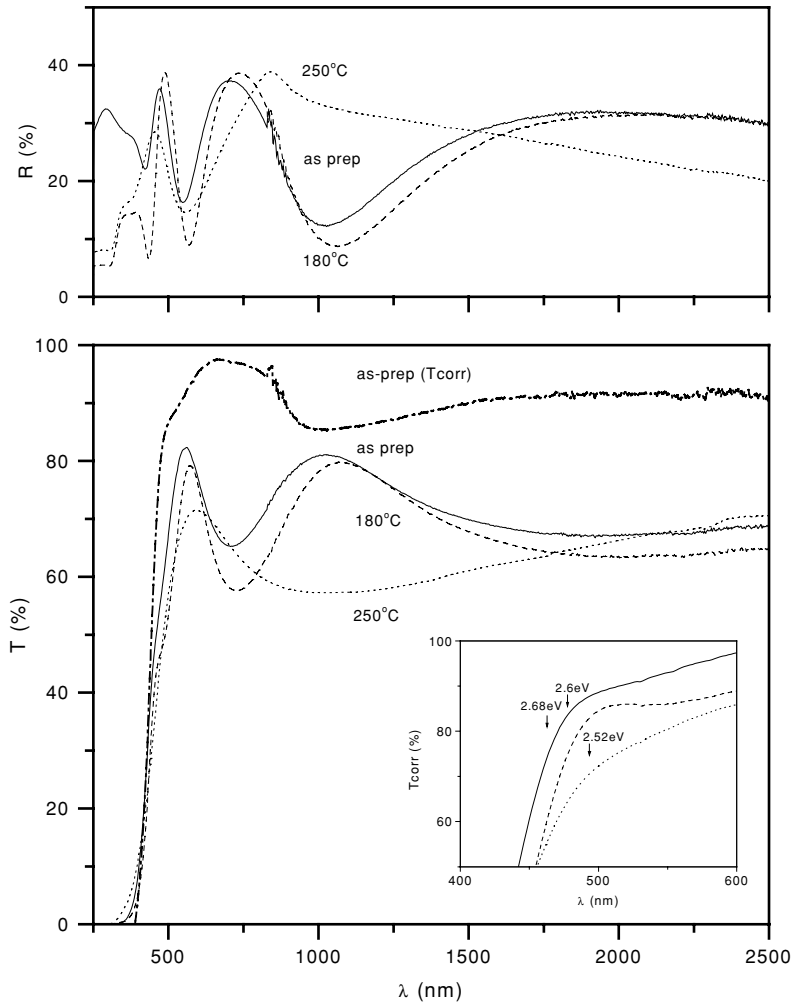

Figure 3. Optical transmittance (T) and specular reflectance (R) spectra of the as-deposited As_2S_3/As_2O_3 film and As_2S_3 film produced through heating the same at 180 and 250 °C. The T_{corr} curves were obtained by correcting the transmittance curves for reflectance loss.

Rigaku D-Max 2000 diffractometer using Cu Kα radiation. A Brucker Equinox 55 FTIR spectrophotometer was used for recording the spectra of the precipitate obtained from the chemical bath dispersed in a KBr pellet. X-ray fluorescence (XRF) spectral data of the as-prepared films were recorded on a Philips MagiX Pro x-ray fluorescence spectrometer with a tube voltage of 60 kV and a current of 60 mA, using an LiF (2 0 0) analyser crystal ($2d$ = 0.403 nm) for As Kα line and a Ge crystal ($2d$ = 0.653 nm) for S Kα line. Optical transmittance and near-normal (5° incidence) specular reflectance spectra of the films were recorded on a Shimadzu UV 3100 PC spectrophotometer with the light beam incident on the film side, against air and a front-aluminized mirror, respectively, as references. The electrical properties of the films were measured on a computerized system consisting of a Keithley 619 electrometer and a Keithley 230 programmable voltage source. Coplanar electrodes of silver paint of 5 mm length at 5 mm separation printed on the surface of the films made the electrical contacts for measuring the dark currents and photocurrents with an applied bias of 10 or 100 V. For the samples in the measuring chamber, sufficient time was given for the current to become steady before recording the measurements: typically for the first 20 s in the dark, the next 20 s under illumination of approximately 1 kW m^{-2} by a tungsten–halogen lamp, and the last 20 s after shutting off the illumination for observing the dark decay. In some cases, a linear four-point probe method was also used to measure the sheet resistance in the films.

3. Results and discussion

3.1. Arsenic sulfide thin films

In nature, arsenic sulfide is present as mineral realgar (pararealgar, As_4S_4, PDF 83-1013, monoclinic), orange-red in colour with a melting point of 307 °C, and as mineral orpiment (As_2S_3, PDF 24-0075, monoclinic), lemon yellow in colour with a melting point of 320 °C [28]. It is also documented in this reference that As_2S_3 is the compound, which is readily formed when an acidified solution of As_2O_3 (present case) reacts with a source of sulfide ions (thiosulfate in the present case). In the present case, the colour of the films and precipitates formed was lemon yellow in daylight. As_2S_3 is known to sublime easily, at temperatures below the melting point, as observed for the films deposited by the present method at temperatures above 250 °C. The sulfide

As_4S_4 may be formed by heating equal atomic amounts of S and As at 500–600 °C and sudden cooling to room temperatures. However, heating could cause changes in the composition of the films; the quantum confinement in semiconductor films can greatly change the optical band gap and consequently the colour of the material, from orange to yellow. In this section, we present the results obtained on chemically deposited arsenic sulfide thin films; issues of structure and composition, and optical and electrical properties are addressed.

Structural properties. Figure 1(*a*) shows the XRD pattern of arsenic sulfide thin films obtained from the bath, recorded at grazing incidence with $\theta = 0.5°$ in a thin film mode. Clearly identifiable peaks of As_2O_3 (arsenolite, PDF 36-1490, cubic) are seen in the pattern along with a broad peak near $2\theta = 18°$. This broad peak may be assigned to reflections from (1 1 1) planes of As_4S_4 with intensity 100% at $2\theta = 17.318°$ and (2 0 0) planes with intensity 25% at $2\theta = 18.035°$ in the PDF standard 83-1013 or to that from (0 2 0) planes of As_2S_3 with intensity 100% at $2\theta = 18.469°$ in the PDF standard 24-0075. When the films were heated at 150, 180 and 250 °C in air in order to enhance crystalline nature, sublimation of the material led to reduction in the thickness of the film: 300 nm (150 °C), 200 nm (180 °C), 170 nm (200 °C) and 150 nm (250 °C). The XRD peaks of crystalline As_2O_3 disappear in these cases and the broad peak still persists. This indicates the reaction of As_2O_3 with available sulfur to form additional As_2S_3. Heating at 300 °C in air or in nitrogen resulted in a total loss of the material from the substrate. In the pattern recorded in the standard mode for the film heated at 250 °C in air, the peaks appearing at 2θ values around 9.6° and 29° match those from (0 1 0) planes of sulfur reported in PDF standard 76-0183 and from (1 3 0) planes with 35% intensity reported for the mineral orpiment in PDF standard 24-0075. We were not able to establish the heat treatment conditions adequate to ascertain the composition of the deposited films as As_2S_3 through XRD analyses.

Figure 1(*b*) shows the infrared spectrum recorded in the 200–600 cm^{-1} region, for the precipitate obtained from the bath dispersed in the KBr pellet. Absorption bands due to As–S stretching vibrations at 389, 361 and 312 cm^{-1} may be identified in this spectrum, based on an earlier reported work [29] on the infrared and Raman spectra of realgar (As_4S_4) and orpiment (As_2S_3). The S–As–S bending vibrations reported at wave numbers <200 cm^{-1} were not studied. If one considers that the thin film has the same chemical composition as that of the precipitate obtained from the same bath, the available infrared data support the XRD results that the thin films formed are of arsenic sulfide.

X-ray fluorescence spectral data of the as-prepared films are shown in figure 2. Using the LiF (200) analyser, the As Kα (10.5 keV) fluorescence emission is detected along with a weaker As Kβ (11.7 keV). With a Ge crystal ($2d = 0.653$ nm), S Kα fluorescence line (2.3 keV) is observed along with the S Kβ line (2.5 keV). Thus, the presence of As and S in the as-deposited films is clearly established through the XRF results. However, we did not investigate the elemental composition in the films to ascertain the composition as As_2S_3 through the use of calibration curves with elemental mixtures. The optical

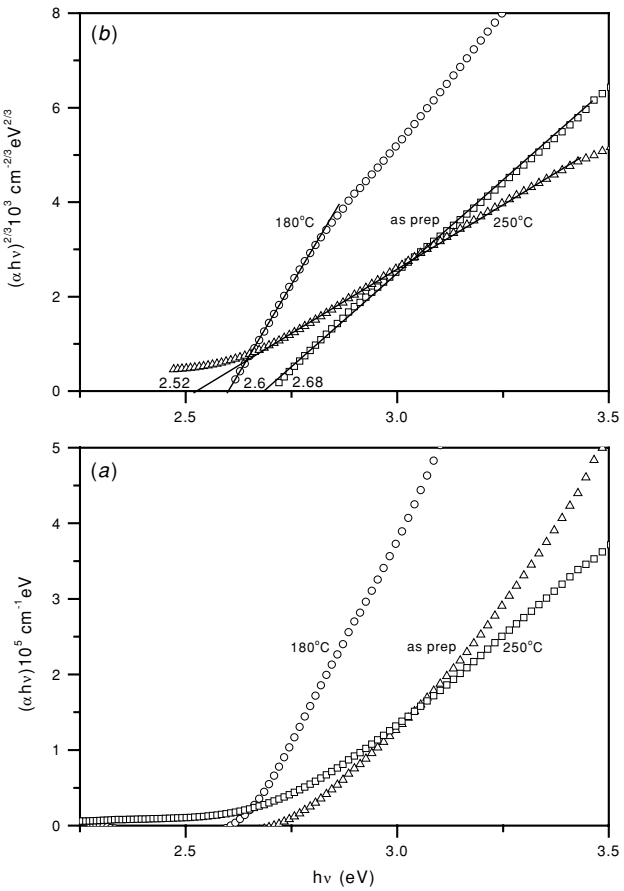

Figure 4. (*a*) $(\alpha h\nu)$ versus $h\nu$ plots for thin films of the as-deposited As_2S_3/As_2O_3 film and As_2S_3 film produced through heating the same at 180 and 250 °C; (*b*) $(\alpha h\nu)^{2/3}$ versus $h\nu$ plots for the films.

characteristics of the films presented below helped to conclude that the films have As_2S_3 as a major component.

3.1.1. Optical and electrical properties. Figure 3 shows the optical transmittance (T) and reflectance (R) spectra of the films: as-prepared (300 nm in thickness), and after heating at 180 °C (200 nm approximately) and at 250 °C (150 nm) in air for 30 min each. At near-infrared wavelengths of the spectra, values of $T + R$ or $T_{corr} = 100T/(100 - R)$ are approximately 90% (shown here for the as-prepared film), which testifies to the specularly reflective surface of the films. In order to evaluate an optical absorption coefficient (α) of the film as a function of the photon energy ($h\nu$), multiple reflections at the air-film and film-substrate interfaces were considered [30]:

$$\alpha = \left(\frac{1}{t}\right) \ln \left[\frac{(1-R)^2 + \sqrt{(1-R)^4 + (2RT)^2}}{2T} \right]. \quad (1)$$

The plots of $(\alpha h\nu)$ versus $h\nu$ for the films were evaluated using the data in figure 3 and are shown in figure 4(*a*). This plot serves as a guideline to determine whether the optical band gap is direct or indirect and whether it involves allowed or forbidden transitions as far as conventional spectroscopic selection rules are concerned. For example, transitions from valence band derived from s-states of individual atoms to conduction band derived from p-states

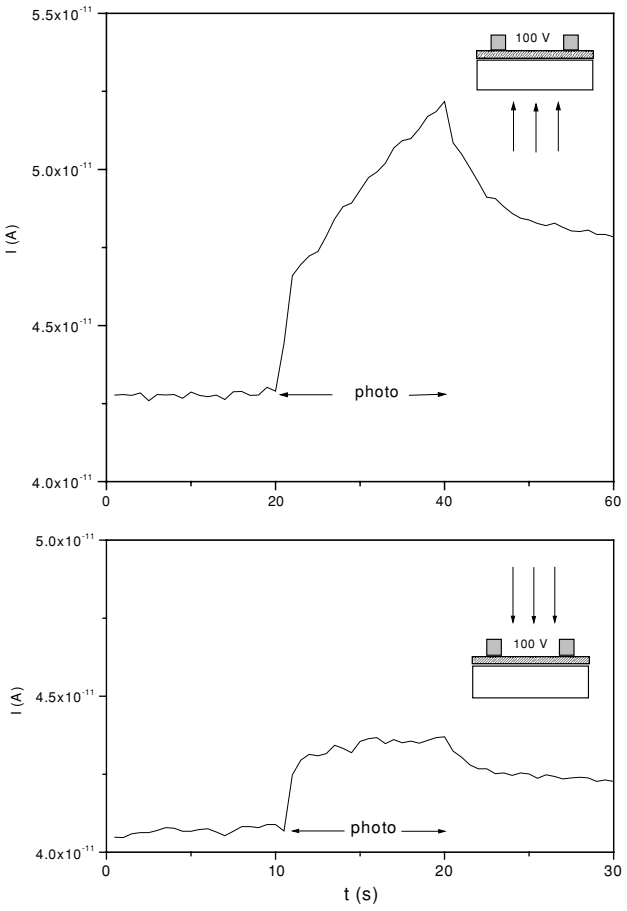

Figure 5. Photocurrent responses in the As_2S_3 film produced by heating at 250 °C in a sulfur-rich atmosphere a chemically deposited film of As_2S_3/As_2O_3, 300 nm in thickness. The mode of illumination is shown.

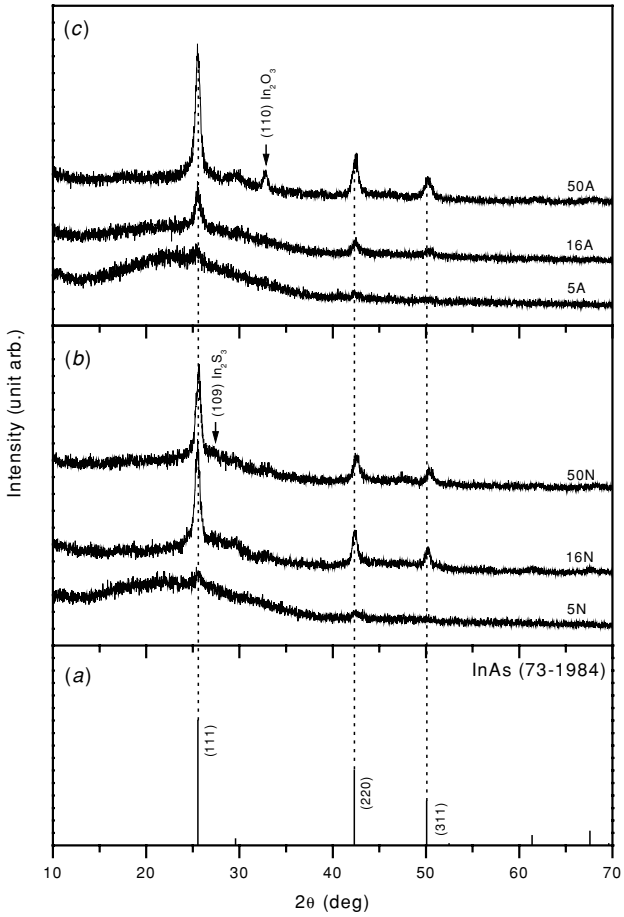

Figure 6. XRD patterns recorded using Cu Kα radiation on thin films with the InAs component formed by heating in nitrogen (N) or air (A) at 250 °C, layers of As_2S_3/As_2O_3–In, with 5, 16 and 50 mg of In used for evaporation. The standard PDF for InAs is given and assignation is made for the dominant peaks of additional crystalline phases.

are allowed, but forbidden if the latter were derived from d-states [31]. However, electronic transitions that are forbidden by spectroscopic selection rules for individual electrons in individual atoms may take place with sufficient probability in other situations, as discussed by Herzberg [32]. In the case of direct transitions (not involving phonons), which are forbidden by conventional selection rules, a plot of $(\alpha h\nu)^{2/3}$ versus $h\nu$ would have a straight line region, the intercept of which on the $h\nu$ axis gives an estimate of a direct band gap. In many cases where direct gaps have been reported, variation of the optical absorption coefficient with photon energy follows a 3/2-law rather than a 1/2-law [31].

One can infer from the data in figure 4(*a*) that in order to obtain a straight line plot, the variation of $(\alpha h\nu)$ with $h\nu$ should be rendered as: $(\alpha h\nu)^{2/3}$ versus $h\nu$ (direct gap, forbidden transition), $(\alpha h\nu)^{1/3}$ versus $h\nu$ (indirect gap, forbidden transitions) or $(\alpha h\nu)^{1/2}$ versus $h\nu$ (indirect gap, allowed transitions). In figure 4(*b*), $(\alpha h\nu)^{2/3}$ versus $h\nu$ plots are given, which offered a straight line fit over the widest range of photon energies. The direct optical gaps obtained from these analyses for arsenic sulfide thin films are as follows: 2.68 eV (as-prepared), 2.6 eV (heated in air at 180 °C) and 2.52 eV (heated in air at 250 °C). The optical band gap of bulk As_2S_3 at 300 K is listed as 2.6 eV (direct) and for As_4S_4, 2.4 eV [11]. The reported band gap values are in agreement with the observed colour of the minerals—yellow for As_2S_3 (mineral, orpiment) and orange for As_4S_4 (mineral, realgar). The as-prepared and heated films reported here are yellow; the optical band gaps of 2.5–2.65 eV obtained from the analysis of the films (figure 4(*b*)) are marked in the inset in figure 3(*a*), on the curves of optical transmittance corrected for reflectance loss. There is a good agreement between the values marked and the onset of strong optical absorption in the films. The observation that the valence band to conduction band excitation is best considered in terms of forbidden electronic transitions with a direct band gap is in agreement with the general behaviour of many semiconductors [31].

Figure 5 shows the photocurrent response under two modes of illumination (as shown) of the films heated in air at 250 °C in a sulfur-enriched atmosphere, measured using a bias of 100 V. From the value of the dark current, a dark conductivity of 10^{-8} Ω^{-1} cm^{-1} is obtained for the material. The photoconductivity of the films is low (also $\approx 10^{-8}$ Ω^{-1} cm^{-1}), but the increase in conductivity due to illumination, from the 10th to 11th s or 20th to 21st s, is clearly observed in both modes of illumination. The electrical conductivity reported for bulk As_2S_3 is extremely low, 10^{-14} Ω^{-1} cm^{-1} [11], but due to imperfections in thin films,

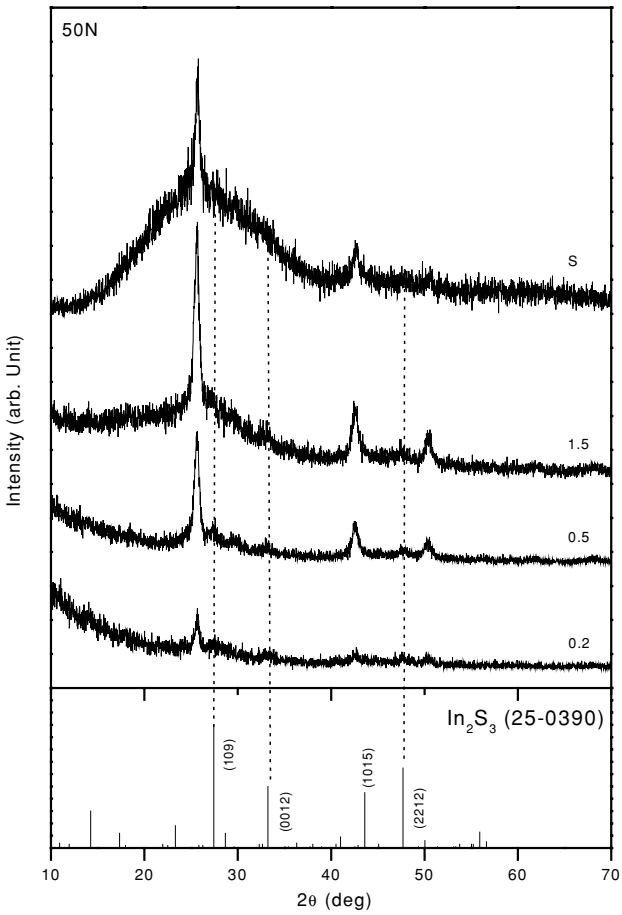

Figure 7. XRD patterns recorded for different angles of incidence ($\theta = 0.2$, etc) of x-rays (Cu Kα) and in the standard mode (S) on the thin film with the InAs component formed by heating in nitrogen (50 N) at 250 °C a layer of As_2S_3/As_2O_3–In. The PDF for In_2S_3 is given to account for the minor phase; the major peaks correspond to InAs, as indexed in figure 6.

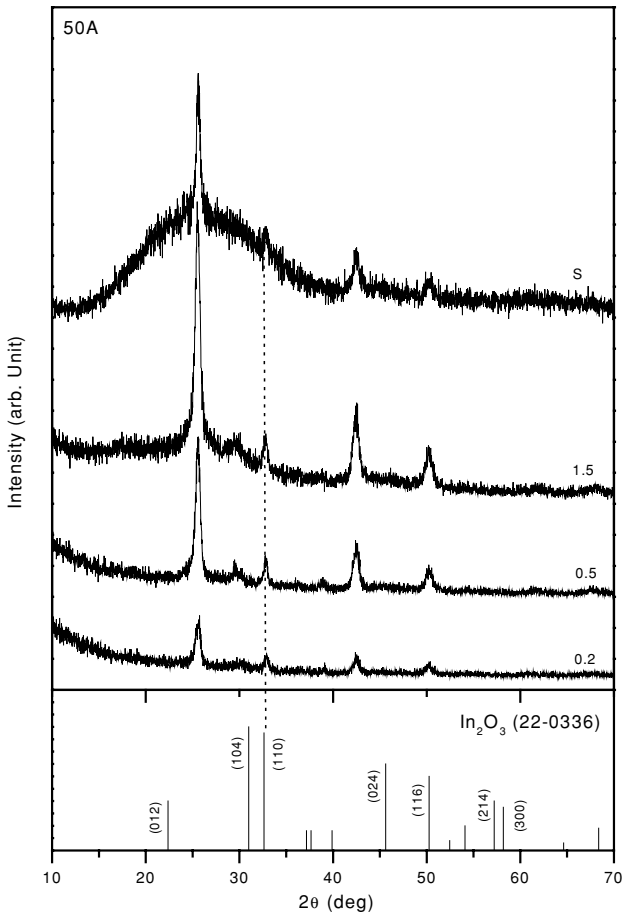

Figure 8. XRD patterns recorded using different angles of incidence of x-rays (Cu Kα) and in the standard mode (S) on the thin film with the InAs component, formed by heating in air (50 A) at 250 °C a layer of As_2S_3/As_2O_3–In. The PDF for In_2O_3 is given to account for the minor phase; the major peaks correspond to InAs, as indexed in figure. 6.

it is usual that a relatively higher value of conductivity is observed for highly resistive materials such as this.

3.2. Formation of InAs by heating of As_2S_3/As_2O_3–In layers

InAs is a III–V compound semiconductor, which crystallizes in a zinc blende structure with a lattice constant 0.60584 nm, with a direct optical gap of 0.36 eV at 300 K and 0.42 eV when extrapolated to 0 K [33]. A major application of this material is in infrared detectors operating in a photovoltaic mode, which offer advantages over photoconductive detectors of PbSe or PbS [34]. The formation of InAs from As_2S_3–In or mixed As_2S_3/As_2O_3–In layers may be possible through reaction of the type

$$As_2S_3 + 2In \rightarrow 2InAs + 3S^{\uparrow}.$$

Using the mass densities of As_2S_3 (3.4 g cm^{-3}) or As_2O_3 (3.7 g cm^{-3}), In (7.3 g cm^{-3}) and InAs (5.8 g cm^{-3}) and the respective formula/atomic masses [35], one can determine that 100 nm of As_2S_3 or As_2O_3 films would require about 40 nm or 60 nm, respectively, of In film for the reactions. The thickness of the InAs films resulting from the reaction would be 95 and 125 nm, respectively. In the present case where the as-deposited films are of mixed composition, the requirement of In for the reaction in As_2S_3/As_2O_3–In layers may be considered as an intermediate to that of As_2S_3 or As_2O_3 thin films. Thus, a complete reaction of As_2S_3/As_2O_3 of 300 nm in thickness would require a thickness of 150 nm of In; the InSb film produced would have a thickness of nearly 330 nm. In the deposition geometry utilized, we have determined that the evaporation of 50 mg of In would suffice for a thickness of 150 nm. Smaller quantities of In—5 and 16 mg—as well were evaporated on As_2S_3/As_2O_3 films to study the evolution of the chemical reaction.

Structural evolution of the layer. Figure 6 gives the XRD patterns recorded in the grazing incidence mode with an angle of incidence $\theta = 1.5^{\circ}$ for the films resulting from heating As_2S_3/As_2O_3–In films at 250 °C for 30 min. The labels 5 N, 5 A, etc denote the amount of In (in mg) evaporated to form a layer and the heating condition—N, nitrogen at 300 mTorr (figure 6(*b*)) and A, air at atmospheric pressure (figure 6(*c*)). The XRD pattern from PDF 73-1984 for InAs is given in figure 6(*a*) for comparison of the 2θ positions and relative intensities of the peaks. Formation of InAs is observed in all the cases, irrespective of the amount of In evaporated and

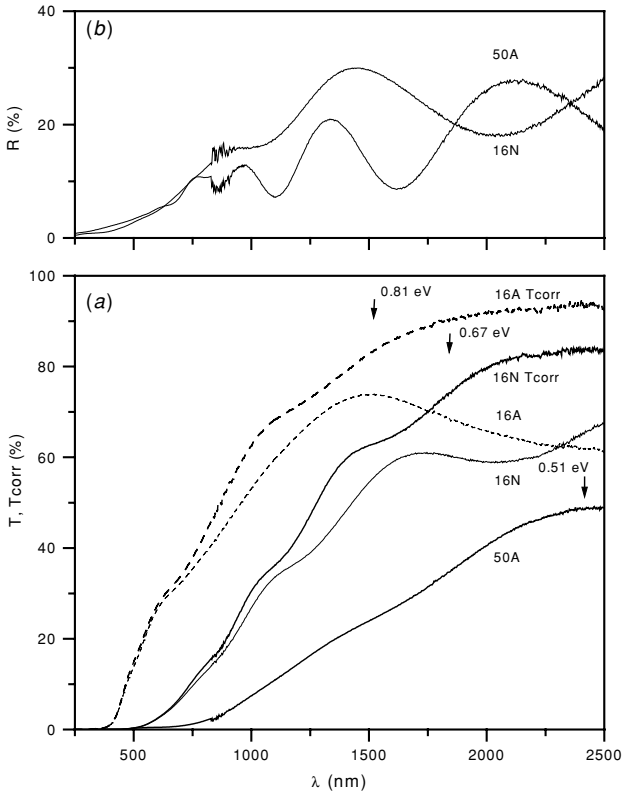

Figure 9. Optical transmittance (T), reflectance (R) and corrected transmittance (T_{corr}) plots for thin films with the InAs component formed by heating in air (16 A, 50 A) or nitrogen (16 N) at 250 °C layers of As_2S_3/As_2O_3–In with 16 or 50 mg of In used in evaporation; the arrows indicate the optical band gap values obtained from figure 10(*c*).

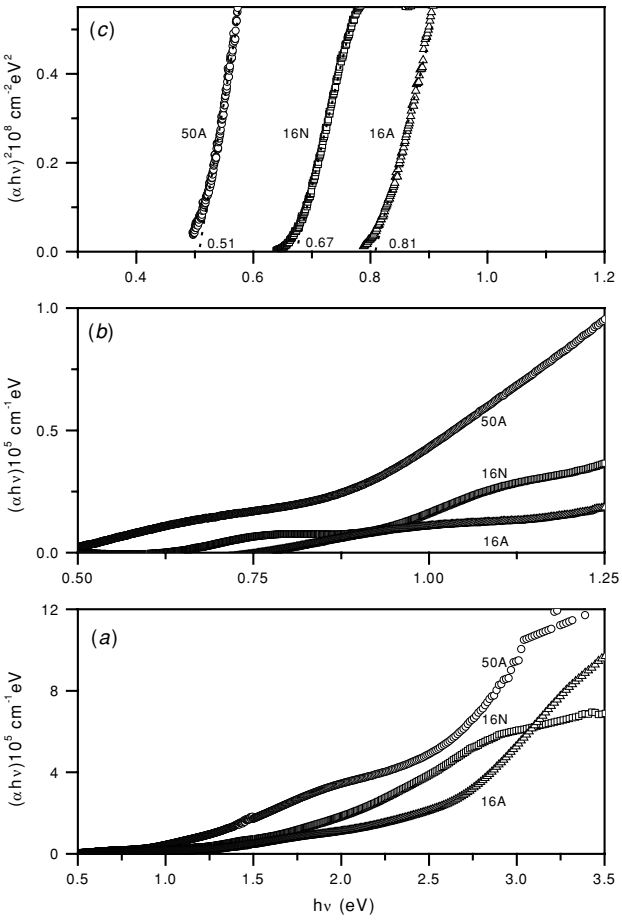

Figure 10. (*a*) ($\alpha h\nu$) versus $h\nu$ plots for thin films with the InAs component formed by heating in air (16 A, 50 A) or nitrogen (16 N) at 250 °C layers of As_2S_3/As_2O_3–In with 16 or 50 mg of In used in evaporation; (*b*) the same plot given for the near-infrared region of photon energies and (*c*) $(\alpha h\nu)^2$ versus $h\nu$ plots for the films.

whether heated in nitrogen or air. In_2S_3 may be present as a minor component in the case of the layers heated in nitrogen; a weak peak appearing at 2θ of 27.46° in figure 6(*b*) may be due to reflection from the (1 0 9) plane of tetragonal indium sulfide reported in PDF 25-039. For sample 50 A, a peak observed at 2θ of 32.8° is attributable to In_2O_3, as assigned in PDF 22-0336 for reflection from the (1 1 0) plane of rhombohedral (Hex) In_2O_3. Peaks due to arsenic sulfide or arsenic oxide (figure 1) are absent in all the patterns.

Figures 7 and 8 show the XRD patterns recorded for the films 50 N and 50 A, respectively, recorded at grazing angles of 0.2°, 0.5° and 1.5° as well as in the standard θ–2θ mode. For the film 50 N, the relative intensity of the XRD peak for the (1 0 9) plane of In_2S_3 with respect to that of the (1 1 1) XRD peak of InAs is as follows: 0.2° incidence, 0.3; 0.5° incidence, 0.15; and 1.5° incidence, 0.05. This confirms that the In_2S_3 layer is stratified near the top of a composite InAs–In_2S_3 layer. In the case of film 50 A, given in figure 8, the relative intensity of the XRD peak for the (1 1 0) plane of In_2O_3 with respect to that of the (2 2 0) XRD peak of InAs is as follows: 0.2° incidence, 0.3; 0.5° incidence, 0.25; and 1.5° incidence, 0.15. The variation here is less drastic. Even in the recording of the XRD pattern in the standard mode, the In_2O_3 peak is clearly noted. This suggests that the film formed as a result of heating As_2S_3/As_2O_3–In in air is a composite film, InAs/In_2O_3, in which the components are rather uniformly distributed throughout the thickness of the film.

Optical and electrical properties. Figure 9(*a*) shows the optical transmittance and reflectance spectra of the films 16 N, 16 A and 50 A, plotted along with T_{corr} curves; figure 9(*b*) shows the specular reflectance curves of the films. It is obvious from the T_{corr} plots that optical absorption sets in at wavelengths in the 2000–2500 nm region for these films, unlike in the case of As_2S_3/As_2O_3 (as-prepared) and As_2S_3 (heated) films shown in figure 3, in which the optical absorption sets in at wavelengths <700 nm. The optical transmittance of unheated As_2S_3/As_2O_3–In (16 and 50 mg) layers is <10% throughout the spectral region, and the reflectance is >60%. Heating at 250 °C either in air or nitrogen causes the indium layer to react with As_2S_3/As_2O_3. Values of $T_{corr} \rightarrow 100\%$ towards wavelength 2500 nm (and above) suggest the absence of a metal film in the layers after the reaction. This was concluded from the XRD patterns discussed above. The arrows placed on the T_{corr} curves represent the optical band gap values evaluated for the InAs component in the film, presented below.

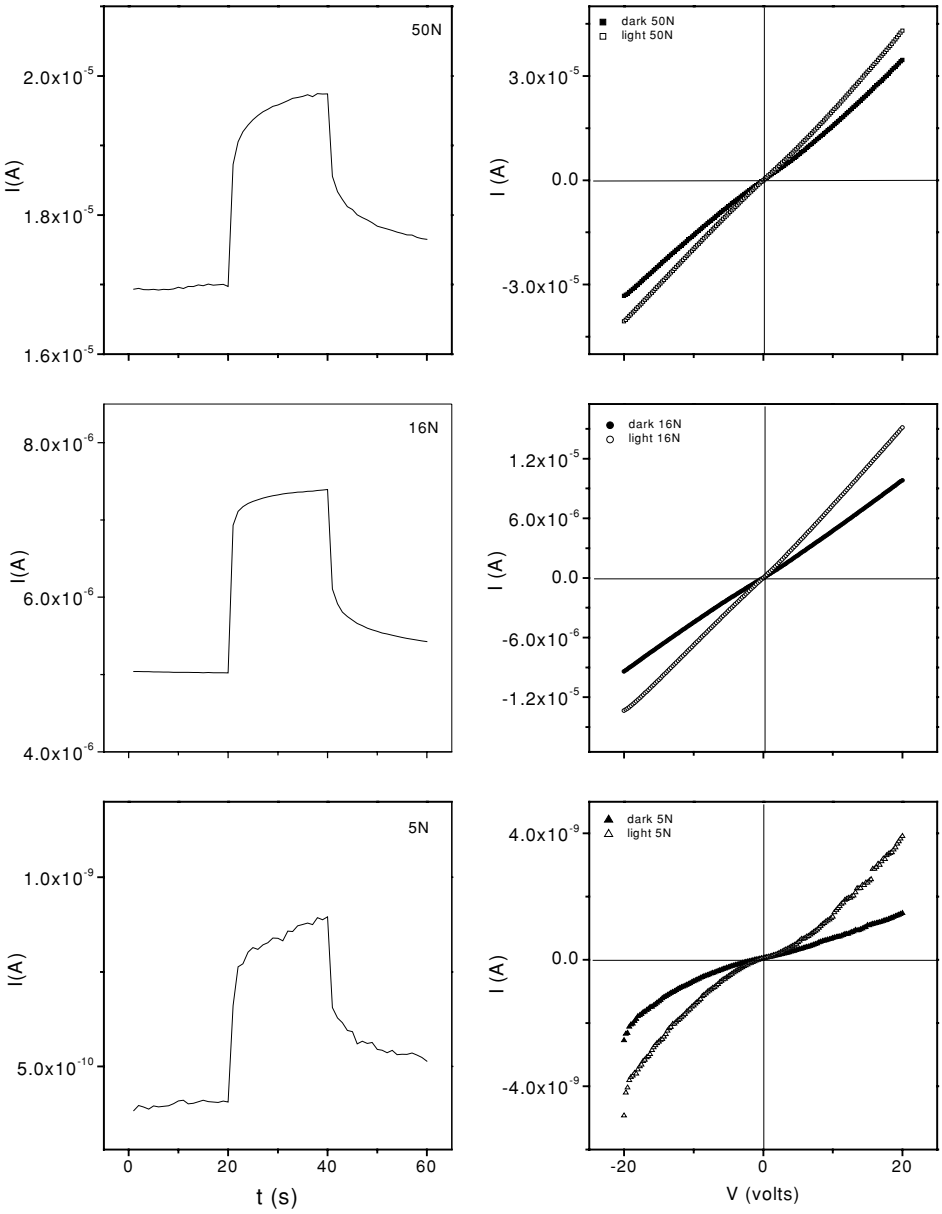

Figure 11. Photocurrent responses under a bias of 10 V of thin films with the InAs component formed by heating in nitrogen at 250 °C layers of As_2S_3/As_2O_3–In with 5, 16 and 50 mg of In used in evaporation. The right side plots are the *I*–*V* curves of the corresponding films.

The plots of $(\alpha h\nu)$ versus $h\nu$ evaluated from the transmittance and reflectance spectra using equation (1) are given in figure 10(*a*). The optical absorption coefficient for the films in the visible region (≈2 eV) is $\approx 10^5$ cm^{-1} and 10^4 cm^{-1} in the near-infrared region (<0.7 eV), described in figure 10(*b*). The reported value of the optical band gap for bulk crystalline InAs is 0.36 eV, and hence the analysis of optical band gap was done for this low energy region. The plots of $(\alpha h\nu)^2$ versus $h\nu$ in figure 10(*c*) exhibit straight line regions with intercepts of 0.51 eV for the sample 50 A, 0.67 eV for the sample 16 N and 0.81 eV for 16 A. The reliability of these estimated values are seen in the T_{corr} plots in figure 9(*a*)—the values approximately correspond to the wavelength where the optical absorption sets in each case. The deviation of these band gap values from those reported for the bulk crystalline material is understood in terms of the quantum confinement effects in polycrystalline grains of 10–30 nm in the InAs component of the films, estimated from the XRD peak width analyses.

Figures 11 and 12 show the photocurrent response measured at a bias of 10 V across pairs of electrodes 5 mm × 5 mm as well as the *I*–*V* characteristics for $V = -20$ V to +20 V, recorded in the dark and under illumination. The following observations could be made.

(1) All the films are photosensitive; the silver print electrodes show ohmic behaviour over a larger range of bias voltage only in the case of thicker films. At the bias of 10 V used for the measurement of photocurrent response, a near-ohmic contact may be assumed.
(2) The presence of In_2O_3 phase in the films prepared by heating in air places the level of dark current and photocurrent to two orders of magnitude higher in samples 50 A compared with 50 N. It is well known

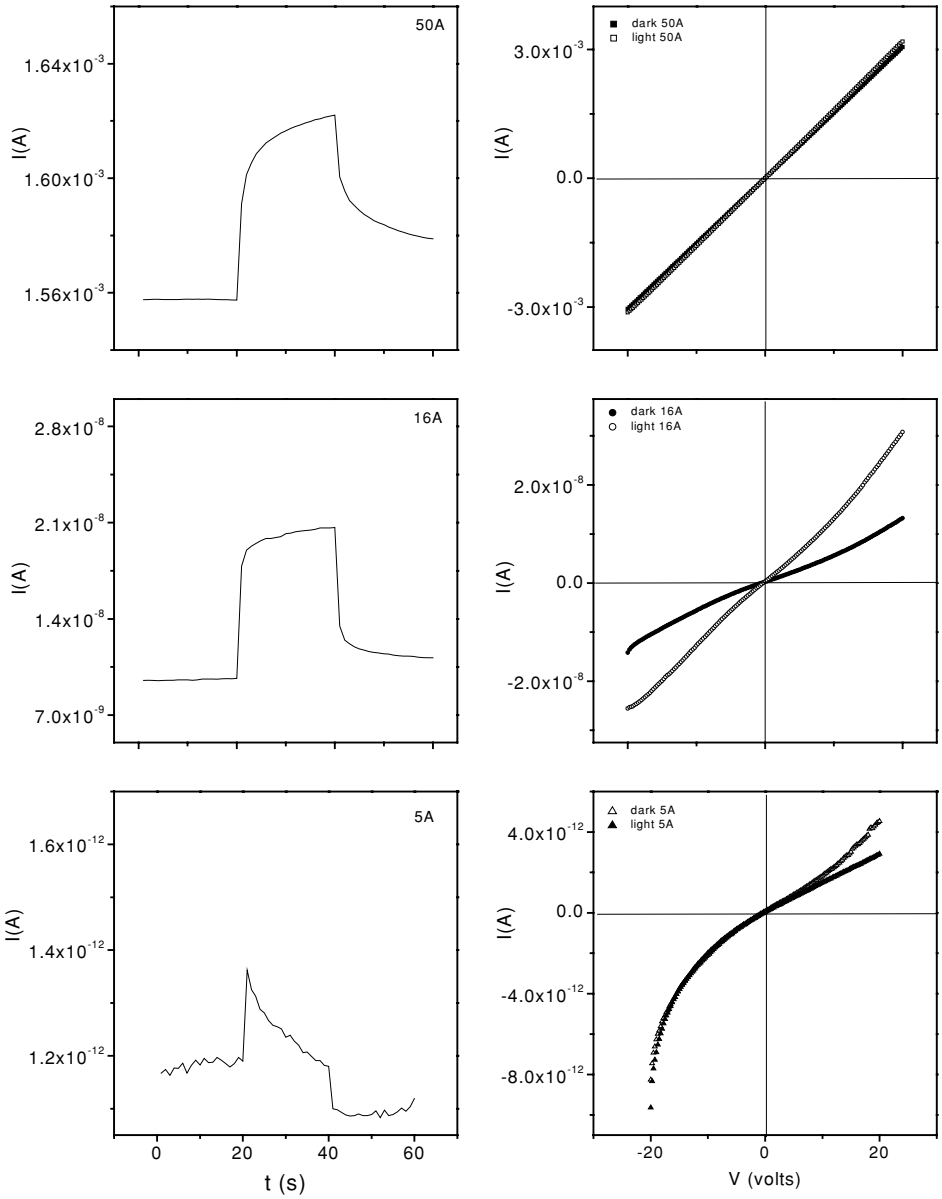

Figure 12. Photocurrent responses under a bias of 10 V of thin films with the InAs component formed by heating in air at 250 °C layers of As_2S_3/As_2O_3–In with 5, 16 and 50 mg of In used in evaporation. The right side plots are the *I–V* curves of the corresponding films.

that In_2O_3:Sn (indium tin oxide, ITO) is a transparent conductive coating with the high electrical conductivity of 10^3–10^4 Ω^{-1} cm^{-1} [36] and that in sub-stoichiometric (In_2O_{3-x}) material, the electrical conductivity can be relatively high, 10^{-2}–10^2 Ω^{-1} cm^{-1}. The latter aspect has been discussed in the case of heated layers of CdSe–In [37] and CdS–In [38]. The In_2O_{3-x} layer with conductivity $\approx$400 Ω^{-1} cm^{-1} was formed by heating the layers at 250 °C in air in those cases. Heating in nitrogen leads to the formation of In_2S_3, as evidenced in the XRD analyses, in which high conductivities as above have not been reported. Hence, InAs would dominate in the electrical conductivity of samples heated in nitrogen. From the data presented in figures 11 and 12, the conductivity of the InAs–In_2O_3 layer 50 A is $\approx$5 Ω^{-1} cm^{-1} and that of the InAs–In_2S_3 layer 50 N is two orders less, $\approx$0.05 Ω^{-1} cm^{-1}.

(3) The formation of InAs is favoured in comparison with that of In_2O_3. In composite films formed in air involving reduced quantities of indium (5 A, 16 A), the electrical current and hence the conductivity is less by about two orders of magnitude compared with those formed in nitrogen. It was seen in the XRD patterns for these samples that formation of InAs precedes that of In_2O_3; XRD peaks of In_2O_3 are not discernible for the samples 5 A and 16 A. While heating the films in air to produce InAs, oxygen is incorporated in grain boundaries, which increases the inter-grain potential barrier, impeding carrier transport. This would reduce the electrical conductivity, compared to InAs formed in nitrogen (5 N, 16 N).

In a 1968 paper, a carrier density of $\approx 10^{24}$ m^{-3} and an electron mobility of 0.3 m^2 V^{-1} s^{-1} were reported for InAs thin films formed by thermal evaporation, which was annealed

at temperatures 300 °C or above [39]. Thus, the electrical conductivity of such films is ≈500 Ω^{-1} cm^{-1}. The electron mobility for bulk crystalline InAs is 3.3 m^2 V^{-1} s^{-1} [33], and the carrier concentration (at 300 K) evaluated for intrinsic material for a band gap of 0.36 eV is only 10^{21} m^{-3}, which suggests that the electrical conductivity of intrinsic InAs is ≈5 Ω^{-1} cm^{-1}. However, a value 0.05 Ω^{-1} cm^{-1} for the sample 50 N obtained here may be accepted as a reliable value for the conductivity of InAs. This is because it has been established through theoretical models supported by experiments that charge carrier mobility and hence the electrical conductivity in polycrystalline materials may be less by one or more orders of magnitude due to chemisorbed oxygen in the grain boundaries [40]. The presence of chemisorbed oxygen in the films would bring down the dark current (conductivity) as well as photocurrent, but the photosensitivity, that is, the ratio of the change in current to dark current would be higher [41]. In some cases, the chemisorption of oxygen utilizes the photo-generated electrons, which would thus cause photocurrent to decrease with time, as seen in the case of sample 5 A in figure 12. In samples where chemisorbed oxygen already exists in the inter-grain region with the associated negative potential, photo-generated holes would neutralize the negative potential. This would lead to an increase in electron mobility and hence an increase in photocurrent during illumination, as observed for samples 16 A and 50 A, and in all cases of InAs produced through heating in nitrogen (figure 11).

4. Conclusions

We have reported here a method to deposit uniform specularly reflective thin films of As_2S_3/As_2O_3 with a possible presence of sulfur, with an overall thickness of 300 nm. Heating the films at temperatures above 150 °C converts the films to As_2S_3. The films show an optical band gap of 2.64 eV (as-prepared) and 2.5–2.55 eV after heating. The films are very resistive; electrical conductivity is ≈10^{-8} Ω^{-1} cm^{-1}. With an In film deposited by evaporation on the as-prepared film followed by subsequent heating in air or nitrogen at 250 °C, InAs forms as the dominant crystalline phase. The optical band gap of the material formed is 0.5–0.8 eV, depending upon the heating conditions. The electrical conductivity of the InAs film formed this way is 0.05 Ω^{-1} cm^{-1}, low in comparison with 5 Ω^{-1} cm^{-1} for intrinsic InAs. For the InAs–In_2O_3 composite film, a conductivity of ≈5 Ω^{-1} cm^{-1} is observed, but this is ascribed to In_2O_3, which is formed along with it. We have found from XRD results and electrical measurements that when an As_2S_3/As_2O_3–In layer is heated at 250 °C, either in air or nitrogen, the readily occurring product is InAs. Formation of the In_2O_3 phase takes place in the layer heated in air or In_2S_3 when heated in nitrogen, only when In is present in excess.

Acknowledgments

We are grateful to Maria Luisa Ramón Garcia for XRD measurements, Patricia Altuzar for XRF measurements and Aaron Sanchez-Juarez for useful discussion. José Campos helped with the electrical measurements and Oscar GomezDaza with optical measurements. Financial support for the project came from DGAPA-UNAM and CONACYT, Mexico.

References

[1] Cimpl Z, Kosek F and Lukes F 1987 *J. Non-Cryst. Solids* **97, 98** 439
[2] Dikova J and Starboa K 2000 *Vacuum* **58** 490
[3] White K, Kumar B and Rai A K 1988 *Thin Solid Films* **161** 139
[4] Santiago J J, Sano M, Hamman M and Chen N 1987 *Thin Solid Films* **147** 275
[5] Yesugade N S, Lokhande C D and Bhosale C H 1995 *Thin Solid Films* **263** 145
[6] Sartale S D and Lokhande C D 2000 *Mater. Res. Bull.* **35** 1345
[7] Mane R S, Sankapal B R and Lokhande C D 2000 *Mater. Chem. Phys.* **64** 215
[8] Rode A V, Zakery A, Samoc M, Charters R B, Gamaly E G and Luther-Davies B 2002 *Appl. Surf. Sci.* **197, 198** 481
[9] Sainov S and Stoycheva-Topalova R 2003 *Vacuum* **69** 365
[10] Smith J D 1973 Arsenic, antimony and bismuth *Comprehensive Inorganic Chemistry* ed J C Bailar, H J Emeléus, R Nyholm and A F Trotman-Dickenson (Oxford: Pergamon) pp 547–621
[11] Madelung O 1992 *Semiconductors other than Group IV Elements and III–V Compounds, in Data in Science and Technology* ed R Poerschke (Berlin: Springer) pp 49–50
[12] Rodríguez-Lazcano Y, Nair M T S and Nair P K 2005 *J. Electrochem. Soc.* **152** G635
[13] Rodríguez-Lazcano Y, Nair M T S and Nair P K 2001 *J. Cryst. Growth* **223** 399
[14] Nair M T S, Peña Y, Campos J, García V M and Nair P K 1998 *J. Electrochem. Soc.* **145** 2113
[15] Bindu K, Campos J, Nair M T S, Sánchez A and Nair P K 2005 *Semicond. Sci. Technol.* **20** 496
[16] Nair M T S, Rodríguez-Lazcano Y and Nair P K 2000 *J. Cryst. Growth* **208** 248
[17] Nair P K *et al* 1998 *Sol. Energy Mater. Sol. Cells* **52** 313
[18] Nair M T S and Nair P K 1990 *Semicond. Sci. Technol.* **5** 1225
[19] Nair P K, Huang L, Nair M T S, Hu H, Meyers E A and Zingaro R A 1997 *J. Mater. Res.* **12** 651
[20] Garcia V M, Nair M T S, Nair P K and Zingaro R A 1997 *Semicond. Sci. Technol.* **12** 645
[21] Rodríguez-Lazcano Y, Peña Y, Nair M T S and Nair P K 2005 *Thin Solid Films* **493** 77
[22] Niesen T P and De Guire M R 2001 *J. Electroceram.* **6** 169
[23] Huang L, Nair P K, Nair M T S, Zingaro R A and Meyers E A 1995 *Thin Solid Films* **268** 49
[24] Fitzgerald A G 1982 *Thin Solid Films* **98** 101
[25] Mittal K L (ed) 1992 *Silanes and Other Coupling Agents* (Utrecht: VSP)
[26] Nair P K, Parmananda P and Nair M T S 1999 *J. Cryst. Growth* **206** 68
[27] Nair P K, Garcia V M, GomezDaza O and Nair M T S 2001 *Semicond. Sci. Technol.* **16** 855
[28] Greenwood N N and Earnshaw A 1984 *Chemistry of the Elements* (Oxford: Pergamon) p 674
[29] Forneris R 1969 *Am. Mineral.* **54** 1062
[30] Schroder D K 1990 *Semiconductor Material and Device Characterisation* (New York: Wiley)
[31] Smith R A 1978 *Semiconductors* (Cambridge: Cambridge University Press) p 313
[32] Herzberg G 1945 *Atomic Spectra and Atomic Structure* (New York: Dover) p 154
[33] Sze S M 1981 *Physics of Semiconductor Devices* (New York: Wiley) p 849
[34] http://www.polytec-pi.fr/Judson/ind_ars-e.htm

[35] Aylward G H and Findlay T J V 1974 *SI Chemical Data* (Milton: Wiley)
[36] Frank G, Kauer E and Köstlin H 1981 *Thin Solid Films* **77** 107
[37] Garcia V M, George P J, Nair M T S and Nair P K 1996 *J. Electrochem. Soc.* **143** 2892
[38] George P J, Sanchez A, Nair P K and Huang L 1996 *J. Cryst. Growth* **158** 53
[39] Howson R P 1968 *J. Phys. D: Appl. Phys.* **1** 939
[40] Orton J W, Goldsmith B J, Chapman J A and Powell M J 1982 *J. Appl. Phys.* **53** 1602
[41] Micheletti F B and Mark P 1967 *Appl. Phys. Lett.* **10** 136